We thank you the reviewer for their suggestions. The response to the reviewers comments are in black while the original comments are in blue.

1. Mathematical notation

1.1 Mathematical symbol names should be single letters (Latin, Greek, or potentially from another alphabet if really needed). Using multi-letter names creates confusion about what is a variable name and what is a multiplication of symbols. This is a convention that very much also holds in the marine biogeochemistry modelling community, for example the NPZD model is named after the conventional (single letter) symbol names for its four prognostic quantities).

Response: The reason we used multiple letters in the equations is to be consistent with the legibility of the code. In the larger framework of the COAWST model where there are several variables, single letter symbols do not suffice.

1.2. If it is necessary or useful to use a multi-letter subscript or superscript to further identify a variable, then this should be typeset in upright letters to avoid the confusion with a product of symbols. Using LATEX, this can be achieved with \mathrm, for example Topt is written as T_{opt}.

Response: We have replaced all the subscripts and superscripts with upright letters. Please see a revised version of Section 2.2 at the end of this response.

1.3. exp is the exponential function, it takes its argument in round brackets and not as an index. e is a number, the base of natural logarithms, and can be exponentiated by writing an index. The current mix of these two notations, for example in equation 2, is at best confusing and at worst meaningless

Response: We have used exp as a function in the equations now with its arguments in brackets.

1.4 . Mathematical function names are typeset upright and usually use lower case letters, for example exp, min ($\exp$, and $\min$ respectively).

Response: We have used lower case letters for all the mathematical functional names (please see revised section 2.2).

1.5 Double subscripts should be avoided where possible. If they are unavoidable then they should not be separated by a hyphen, because a horizontal line universally means subtraction. A comma, possibly augmented by brackets of some type, would be a better choice.

Response: We have eliminated hyphen as per the review and used a comma to describe the double subscripts.

2. Equations and discretisation

The introduction to section 2.2 claims that the remainder of the section will introduce the equations solved. In fact, we are only treated to a disconnected set of source terms for an unspecified set of equations. Please provide the full set of differential equations being solved, before going into detail about the definition of the terms. In addition, the equations are clearly being solved numerically, so a complete model description also requires the inclusion of the discretisation used, and how the resulting discrete linear or nonlinear system is solved.

Response: We would add a modified section 2.3 for connecting the SAV growth model that provides the source terms to the complete model description. It mentions the integration of source terms into the water-column biogeochemistry model and the discretization methods of the resulting system of equations.

3. Verification and evaluation There is effectively no verification or validation of the model. The test cases provided are purely descriptive: the model is run and the authors describe what happened. This does not provide suitable

evidence either that the model is correctly implemented, or that it is realistic. The usual way of demonstrating the former would be using the method of manufactured solutions (MMS) to create artificial analytical solutions to the system, and then demonstrating convergence to them at the expected rate. For more information on MMS see Farrell et al. (2011) section 4.1 (https://doi.org/10.5194/gmd-4-435-2011).
In order to provide some level of evaluation of the model, it would be necessary to present a qualitative or quantitative comparison of the model to an external reference. The external reference might be directly with observational data, or might be with the results of another well-evaluated model. In any event, an external comparator is absolutely necessary.

Response:
3.1 Verification
The process of manufactured solutions to create artificial analytical solutions is possible where an analytical solution of a physical problem is available and convergence of the solution to the partial differential equation can be tested. The authors acknowledge that similar verification ideas are the way to validate test cases. In the current work, we used modified an existing point model (Madden and Kemp, 1996) that calculated changes in vegetation biomass that we have adapted to predict changes in vegetation properties (density and height) that impact physical processes in the model (e.g., advection, resuspension). The point model was implemented with the inclusion of spatial variation in the 3-D model. There is no analytical solution to the point model that we developed and we can only verify the implementation of a point model in the 3-D framework by running the point model separately and running the 3-D model after turning off the hydrodynamics, sediment dynamics along with the advection-diffusion processes (i.e. stripping the 3-D model down to be a point model). Alternatively, the idealized domain can be utilized within the 3-D model to show the sensitivity of using individual components of the model for eg. turning the sediment model off to show that a better light climate can provide better environment for SAV to grow. The overarching goal of the idealized case in the manuscript is to demonstrate that the model is capable of simulating expected dynamics that included process of seagrass growth and dieback, its effect on sediment and hydrodynamics processes (i.e. two way feedback between the hydrodynamics-sediment-biological) dynamics. However, in lieu of this type of evaluation of the model, we are in the revised manuscript providing a comparison of modeled vegetation properties with independently-collected field data for the case of West Falmouth Harbor. In order to do build this qualitative (SAV distribution) and quantitative (SAV biomass at specific locations) comparison with external data, we will incorporate a new section (Section 4.3) to perform the model evaluation. Typically, the coupled biological-sediment models are assessed in a similar manner (Matsumoto et al., 2013, Cossarini et al. 2017, Sherwood et al., 2018).

Below are the sections that we plan to include in the revised sections (Section 2.2, Section 2.3, and Section 4.3).

2.2 SAV growth model

The SAV growth model is primarily based upon a previous growth model developed and implemented in Chesapeake Bay by Madden and Kemp (1996). The model simulates the temporal dynamics of above ground biomass (AGB) that consists of stems or shoots, and the below ground biomass (BGB) that consists of roots or rhizomes. In addition to AGB and BGB, epiphytic algal biomass (EPB) is simulated to account for reductions in light availability to plant leaves due to shading of SAV leaves by epiphytes under high nutrient loading conditions. AGB, BGB and EPB are simulated as total biomass per unit area, with nitrogen as the currency for biomass. Changes in AGB and BGB pools are simulated as a function of primary production and respiration, mortality (e.g., grazing), and nitrogen exchange through the seasonal translocation of nitrogen between roots and shoots. EPB are modelled as a function of primary production, respiration, and mortality.

The remaining section describes the source terms that calculate the evolution of AGB, BGB and EPB. The default input parameters required by the following model equations are described in Table 1.

2.2.1 Primary production (pp_{SAV}): The primary production of AGB depends on the maximum potential growth rate (ua) and downward deviations from this maximal rate resulting from light ($llmt_{\mathrm{SAV}}$) and nutrient ($nlmt_{\mathrm{SAV}}$) availability as:

$$pp_{\mathrm{SAV}} = ua \min(lmt_{\mathrm{SAV}}, nlmt_{\mathrm{SAV}}) \quad (1)$$

The maximum potential growth (ua) can be described as:

$$ua = \lambda_{\mathrm{SAV}}\, nlmt_{\mathrm{SAV}}\, scl \exp[arc\, \left(\frac{1.0}{T-T_{\mathrm{opt}}}\right)] \quad (2)$$

where λ_{SAV} is a self-shading parameter that accounts for crowding and self-shading within the SAV canopy, scl accounts for SAV's maximum growth fraction, arc is the active SAV respiration coefficient, T is the temperature in water column, T_{opt} is the user defined optimum temperature that allows for species-specific sensitivities to temperature. The self-shading parameter, λ_{SAV} used in Eq. 3 is calculated by setting a maximum aerial biomass of SAV (Madden and Kemp 1996), thereby making growth rates density-dependent and is defined as:

$$\lambda_{SAV} = 1 - \left(\frac{AGB}{\lambda_{\mathrm{SAV,max}}}\right)^2 \quad (3)$$

where AGB is the above ground SAV biomass and $\lambda_{\mathrm{SAV,max}}$ accounts for the maximal SAV biomass.

The availability of photosynthetically active radiation (PAR) for SAV leaves in the bottom cell is simulated using a bio-optical model (Gallegos et al. 2009, del Barrio et al. 2014). While the bio-optical model generates predictions of light available across the spectrum within PAR, the light availability ($llmt_{\mathrm{SAV}}$)used to compute primary production (Eq. 1) is obtained through traditional photosynthesis-irradiance curves based on total PAR used to represent SAV growth responses to light:

$$llmt_{\mathrm{SAV}} = \frac{PAR}{klmt+PAR} \quad (4)$$

where $klmt$ is the half-saturation for light limitation for SAV and PAR refers to photosynthetically available radiation that is obtained from the bio-optical model.

The nutrient limitation ($nlmt_{\mathrm{SAV}}$) required in Eq.1 to compute primary production represents the fact that rooted plants can obtain nutrients from both sediments (as in Madden and Kemp, 1996) and the water-column and is defined as:

$$nlmt_{\mathrm{SAV}} = DIN_{\mathrm{wc}} + \frac{kn_{\mathrm{t}} DIN_{\mathrm{sed}}}{kn_{\mathrm{wc}} DIN_{\mathrm{sed}} + kn_{\mathrm{t}} DIN_{\mathrm{sed}}} \quad (5)$$

where DIN_{wc} is the dissolved inorganic nitrogen concentration in the water column based on the sum of NH4 (Ammonium) and NO3 (nitrate) in the water column and DIN_{sed} is the amount of dissolved inorganic nitrogen (DIN = NH4 + NO3) in the sediment bed layer, and kn_{t} is the half-saturation for nutrient limitation for SAV roots.

2.2.2 Respiration: SAV respiration terms are partitioned into active and basal respiration, where the active respiration term represents respiration that is dependent on the photosynthesis rate, and the basal rate represents maintenance respiration rate.

The active respiration term is defined as:

$$agar_{\mathrm{SAV}} = pp_{\mathrm{SAV}}\, arsc \exp(arc\, T) \quad (6)$$

where pp_{SAV} is the primary production term (Eq. 1), $arsc$ is the maximum fraction of photosynthesis available for respiration, arc is the SAV's active respiration coefficient, T is the temperature in the water column.

The above ground basal respiration term is defined as:

$$agbr_{\mathrm{SAV}} = bsrc \exp(rc\ T) \tag{7}$$

where $bsrc$ is the maximum fraction of SAV below ground biomass (BGB) that is respired, rc is the SAV basal respiration coefficient for both AGB and BGB, T is the temperature in the water column.

2.2.3 Mortality: The mortality of SAV is computed separately for above-ground and below-ground biomass, where AGB mortality accounts for the sloughing of leaves and grazing in combination as:

$$agm_{\mathrm{SAV}} = (km_{\mathrm{ag}}\ AGB)^2 \tag{8}$$

where km_{ag} is the above ground SAV mortality rate (sloughing).

Below ground mortality, bgm_{SAV}, is a function of temperature and is given as:

$$bgm_{\mathrm{SAV}} = 0.01\ BGB \exp(km_{\mathrm{bg}}\ T) \tag{9}$$

where km_{bg} is the below-ground SAV mortality rate.

Additional terms include that modify the AGB and BGB include the seasonal exchange (translocation) of root material (nitrogen) quantified as a fraction of primary production and the translocation of BGB to AGB which represents the seasonal translocation of nitrogen from roots to stems as the plants initially emerge in spring. Each of these terms is initiated on a specified day of the year (Madden and Kemp 1996), and can be altered to account for species differences or regional differences in the physiology of particular species.

The epiphyte biomass (EPB) is computed similarly to SAV biomass by simulating EPB as a function of primary production, respiration, and mortality (e.g., grazing).

2.2.4 Primary production (pp_{EPB}): The primary production of EPB depends on the maximum potential growth rate (ua_{EPB}) and a limitation between light ($llmt_{\mathrm{EPB}}$) and nutrient ($nlmt_{\mathrm{EPB}}$) availability, as:

$$pp_{\mathrm{EPB}} = ua_{\mathrm{EPB}} \min(llmt_{\mathrm{EPB}}, nlmt_{\mathrm{EPB}}) \tag{10}$$

The maximum potential growth of EPB (ua_{EPB}) can be described as:

$$ua_{\mathrm{EPB}} = \lambda_{\mathrm{EPB}}\ nlmt_{\mathrm{EPB}}\ scl_{\mathrm{EPB}} \exp[arc_{EPB}\ \left(\frac{1.0}{T - T_{\mathrm{EPB,opt}}}\right)] \tag{11}$$

where λ_{EPB} is the self-shading parameter that accounts for spatial limits on the epiphyte population, scl_{EPB} accounts for epiphyte's maximum growth fraction, arc_{EPB} is the T is the temperature in water column, $T_{\mathrm{EPB,opt}}$ is the user defined optimum temperature that allows for species-specific sensitivities to temperature. λ_{EPB} is calculated by setting a maximum aerial biomass of EPB, thereby making growth rates density-dependent similar to the SAV growth rate, as:

$$\lambda_{\mathrm{EPB}} = 1 - \left(\frac{EPB}{\lambda_{\mathrm{EPB,max}}}\right)^2 \tag{12}$$

where EPB is the epiphyte biomass and $\lambda_{\mathrm{EPB,max}}$ is the maximum epiphyte biomass.

The light availability ($llmt_{\mathrm{EPB}}$) used to compute primary production (Eq. 10) is obtained through traditional photosynthesis-irradiance curves used to represent epiphyte growth response to light, as:

$$llmt_{\mathrm{EPB}} = \frac{PAR}{kl_{\mathrm{EPB}} + PAR} \tag{13}$$

where kl_{EPB} is the half-saturation for light limitation for epiphytes and PAR is the photosynthetically available radiation obtained from the bio-optical model.

The nutrient limitation ($nlmt_{\mathrm{EPB}}$) required in Eq.1 to compute primary production for epiphytes depends only on the nutrients in the water-column and is a traditional algal form (e.g., Monod model) given as:

$$nlmt_{\mathrm{SAV}} = \frac{kn_{\mathrm{EPB}} DIN_{wc}}{kn_{\mathrm{EPB}} DIN_{\mathrm{wc}} + kn_{\mathrm{EPB}}} \tag{14}$$

where DIN_{wc} is the amount of dissolved inorganic nitrogen in the water column, kn_{EPB} is the half-saturation for nutrient limitation for epiphytes.

2.2.5 Respiration: Epiphyte respiration terms are partitioned into active and basal respiration, where the active respiration term represents respiration that is dependent on the photosynthesis rate, the basal rate represents the maintenance respiration rate.

The active respiration term is defined as:

$$aresp_{\mathrm{EPB}} = pp_{\mathrm{EPB}}\ arsc_{\mathrm{EPB}} \exp(arc_{\mathrm{EPB}}\ T) \tag{15}$$

where pp_{EPB} is the primary production term (Eq. 1), $arsc_{\mathrm{EPB}}$is the maximum fraction of photosynthesis for epiphytes, arc_{EPB} is the epiphyte's active respiration coefficient, T is the temperature in the water column.

The basal respiration term is defined as:

$$bresp_{\mathrm{EPB}} = bsrc_{\mathrm{EPB}} \exp(rc_{\mathrm{EPB}}\ T) \tag{16}$$

where $bsrc$ is the maximum fraction of epiphyte biomass that is respired, rc is the epiphyte basal respiration and T is the temperature in the water column.

2.2.6 Mortality: The mortality of epiphytes depends on mortality and grazing of algal cells, as well as losses associated with SAV sloughing (which effectively removes epiphytes from a cell).

The mortality term is given as a simple linear form:

$$mort_{\mathrm{EPB}} = kmort_{\mathrm{EPB}} EPB \tag{17}$$

where $kmort_{\mathrm{EPB}}$ is the epiphyte mortality rate.

The loss of epiphyte biomass due to grazing ($\mathrm{grz}_{\mathrm{EPB}}$) modelled using an Ivlev function can be described as:

$$grz_{\mathrm{EPB}} = grz_{\mathrm{EPB,max}}(1.0 - \exp(-grz_{EPB})) \tag{18}$$

where $grz_{\mathrm{EPB,max}}$ is the maximum grazing rate on epiphytes and grz_{EPB} is the grazing coefficient on epiphytes.

The reduction of epiphyte biomass due to the SAV sloughing loss is computed as:

$$EPB_{\mathrm{SAV,slgh}} = \left(\frac{agm_{\mathrm{SAV}}\, dtdays}{AGB}\right) \quad (19)$$

where agm_{SAV} is the above ground mortality term described in Eq. 8, is the time step size in per day units and AGB is the above ground biomass.

The above ground biomass (AGB) computed in the SAV growth model is utilized to obtain SAV shoot height (meters) and stem density (stems/m^2), to allow for the biomass model (AGB) to be translated into variables input into the SAV-hydrodynamic coupling. The shoot height (l_v) is related to AGB as:

$$l_{\mathrm{v}} = 45 + \left(\frac{AGB_{\mathrm{SAV}}}{100+AGB_{\mathrm{SAV}}}\right) \quad (20)$$

The relationship is based on measurements of *Zostera marina* in Chincoteague Bay and Chesapeake Bay (Fig. 2), but is consistent with relationships for *Z. marina* determined elsewhere (Krause-Jensen et al., 2000). Other three-dimensional models have used similar formulations (e.g., Cerco and Moore, 2001 for Chesapeake Bay).

SAV stem density n_{v}, (in stems/m^2) is computed from a similar empirical formulation based on relationships in Krause-Jensen et al., 2000 and is computed as:

$$n_{\mathrm{v}} = 4.45\, AGB_{\mathrm{SAV}} \quad (21)$$

2.3 Integration of SAV growth model with Water-Column Biogeochemistry Model (BGCM model)

The SAV growth model is built to interact dynamically with the water-column biogeochemistry model (BGCM model) within the COAWST modelling framework. We utilize one of the existing BGCM models developed by Fennel et al., 2006 that accounts for nutrients (NO_3, NH_4), phytoplankton and zooplankton biomass, and detritus. The spectral irradiance model that provides the light attenuation in response to chlorophyll, sediment, and CDOM was previously integrated (Gallegos et al. 2009, del Barrio et al. 2014) into the BGCM model. Along with the light attenuation model, the effects of algal respiration, seagrass kinetics and diel oxygen dynamics were also added to BGCM model. The BGCM model was implemented within the hydrodynamic component of COAWST model, ROMS (Regional Ocean Modeling System). ROMS is a three-dimensional, free surface, terrain-following numerical model that solves finite-difference approximations of the RANS equations using the hydrostatic and Boussinesq assumptions (Chassignet et al., 2000 and Haidvogel et al., 2000). ROMS is discretized in horizontal dimensions with curvilinear orthogonal Arakawa C grid (Arakawa, 1966). The tracer concentrations are calculated at the grid cell centers. The BGCM model in the current simulations solved for twelve state variables. Each state variable is calculated based on the tracer transport equation is as follows:

$$\frac{\partial C}{\partial t} + u\frac{\partial C}{\partial x} + v\frac{\partial C}{\partial y} + w_d\frac{\partial C}{\partial z} = \frac{\partial}{\partial z}\left(v\frac{\partial C}{\partial z}\right) + C_{source} \quad (22)$$

where *C* is the tracer quantity, *t* is time, *x* and *y* are the horizontal coordinates and *z* is the vertical coordinates. *u* and *v* are the horizontal components of current velocity with w_d being the sinking velocity for tracers such as detritus. v is the turbulent diffusivity coefficient and C_{source} is the tracer source/sink term, which represents the net effects of all sources and sinks in this representation. There are several choices of advection schemes for tracer advection available in COAWST (Kalra et al., 2019) and in the current simulations, we utilized Multidimensional Positive Definite Advection Transport Algorithm (MPDATA) scheme (Smolarkiewicz, 1984) that has been derived from Lax Wendroff (LW) family of schemes. The time marching scheme for tracers involves a predictor-corrector step using the leapfrog-trapezoidal methods. The 3-D tracer equations are solved at a different and shorter time step than the depth-integrated 2-D barotropic equations. The integration between the baroclinic mode and barotropic mode is performed using a split-explicit time step approach (Shchepetkin and McWilliams, 2005, 2009). The predictor step calculates the tracer

values that updates the momentum equations at an intermediate time step. At that point, the split-explicit algorithm is executed and the update of tracers is done using the corrector step after the new values of velocity are available. For more details of this algorithm, readers are readers are referred to Shchepetkin and McWilliams, 2005 and 2009. The vertical tracer diffusion terms are solved using a fourth-order centered scheme (Shchepetkin and McWilliams, 2005). The vertical advective fluxes are computed using the piecewise parabolic method (Colella and Woodward, 1984). The vertical terms utilize a backwards Euler method for time marching.

The changes in water-column variables (dissolved and particulate nitrogen, dissolved oxygen, dissolved inorganic carbon) due to the SAV growth model occur locally at the bottom cell through the source terms (C_{source}) that affect six state variables in the BGCM model: NO3 (Nitrate), NH4 (Ammonium), DO (Dissolved Oxygen), CO2 (Carbon dioxide), LDeN (Labile Detrital Nitrogen), LDeC (Labile Detrital Carbon). The change in these state variables based on the SAV growth model is as follows:

$$\frac{\partial DIN_{SAV}}{\partial t} = (agar_{\mathrm{SAV}} + agbr_{\mathrm{SAV}} - pp_{\mathrm{SAV}})(1 - sed_{\mathrm{frc}})dtdays + (aresp_{\mathrm{EPB}} + bresp_{\mathrm{EPB}} - pp_{\mathrm{EPB}})dtdays \quad (23)$$

where $\frac{\partial DIN_{SAV}}{\partial t}$ is the net impact of SAV and epiphyte growth on water-column nitrogen concentrations and sed_{frc} decides the portioning of nutrient uptake between sediment and water column using a logistic function and is defined as:

$$sed_{\mathrm{frc}} = 1 - \left(\frac{1}{1+\exp[-mx_{\mathrm{frc}}(DIN_{\mathrm{wc}} - ks_{\mathrm{frc}})]}\right) \quad (24)$$

where mx_{frc} and ks_{frc} are constants and equal to 0.2 and 15.0 respectively and DIN_{wc} (dissolved Inorganic Nitrogen) is calculated as a sum of state variables NH4 (Ammonium) and NO3 (nitrate) in the water column. If net growth from SAV and epiphytes is negative, the net nitrogen regeneration is realized as NH4 production in the water column ($\frac{\partial NH4}{\partial t} = \frac{\partial DIN_{SAV}}{\partial t}$). If there is net growth originating from SAV and epiphytes, the associated water column uptake of DIN is apportioned between NO3 and NH4 in proportion to their availability in the water-column via the following equations:

$$\frac{\partial NH4}{\partial t} = \left(\frac{\partial DIN_{SAV}}{\partial t}\right)\left(\frac{NH4}{DIN_{WC}}\right) \quad (25)$$

$$\frac{\partial NO3}{\partial t} = \left(\frac{\partial DIN_{SAV}}{\partial t}\right)\left(\frac{NO3}{DIN_{WC}}\right) \quad (26)$$

$$\frac{\partial DO}{\partial t} = (pp_{\mathrm{SAV}} - agar_{\mathrm{SAV}} - agbr_{\mathrm{SAV}} + pp_{\mathrm{EPB}} - aresp_{\mathrm{EPB}} - bresp_{\mathrm{EPB}})dtdays \quad (27)$$

$$\frac{\partial CO2}{\partial t} = (agar_{\mathrm{SAV}} + agbr_{\mathrm{SAV}} - pp_{\mathrm{SAV}} + aresp_{\mathrm{EPB}} + bresp_{\mathrm{EPB}} - pp_{\mathrm{EPB}})dtdays \quad (28)$$

$$\frac{\partial LDeN}{\partial t} = (agm_{\mathrm{SAV}} + mort_{\mathrm{EPB}} + grz_{\mathrm{EPB}})dtdays \quad (29)$$

$$\frac{\partial LDeC}{\partial t} = (agm_{\mathrm{SAV}} + mort_{\mathrm{EPB}} + grz_{\mathrm{EPB}})dtdays \quad (30)$$

All the source terms in equations (23 and 25-30) are solved using the SAV growth model described in Section 2.2 and in equation 28 and 30, these terms are converted to moles of Carbon from moles of Nitrogen assuming a fixed (and user-defined) C:N ratio in SAV tissue (we assumed a C:N of 30).

Section 4.3. Model evaluation in West Falmouth Harbor

In order to qualitatively evaluate the seagrass growth model, we have compared the modeled results with observations by del Barrio et al. (2014) that measured the extent of seagrass coverage in West Falmouth Harbor (red outline in Fig. 11). The field data is only available for the northern region of WFH where the model-data comparisons are performed. The model results are compared by extracting the peak above ground biomass (AGB) on 14th day of the simulation and normalized with the initial above ground biomass. The ratio of $AGB/AGB_{initial}$ is considered as a representative of seagrass growth. We assume that for $AGB/AGB_{initial} > 1$, there is a potential for seagrass growth and for $AGB/AGB_{initial} <1$, the conditions are unfavorable for seagrass growth. In fig 11, the model and field data show a 89% agreement to determine the seagrass growth or dieback. The western region of outer harbor shows seagrass growth potential and agrees with the extent that the seagrass coverage is observed. In the eastern region, the field data shows no seagrass coverage and the model also predicts potential seagrass dieback. The model predicts seagrass dieback because of nitrate loading from shoreline point sources that leads to increased chlorophyll and light attenuation (figures 8a, b). The model and observations do not compare well in the central basin of outer harbor where the model shows seagrass dieback potential while the field data shows presence of seagrass. In the central basin, the field data shows the presence of seagrass while its density remains low in this region. On the other hand, the modelled seagrass suffers dieback due to the bathymetric controls in the deeper central basin (decreased near-bottom PAR Fig. 8c).

Although direct estimates of above ground biomass are not available for West Falmouth Harbor, the model range of 0-114 mmol N m^{-2} is consistent with annual mean *Z. marina* biomass (10-88 mmol N m^{-2}) reported in nearby shallow systems on Cape Cod (Hauxwell et al. 2003) assuming a literature-based average that above ground SAV biomass is 1.5% N. The range in the model is computed based on the minimum and maximum values of AGB during the 18 day simulation period.

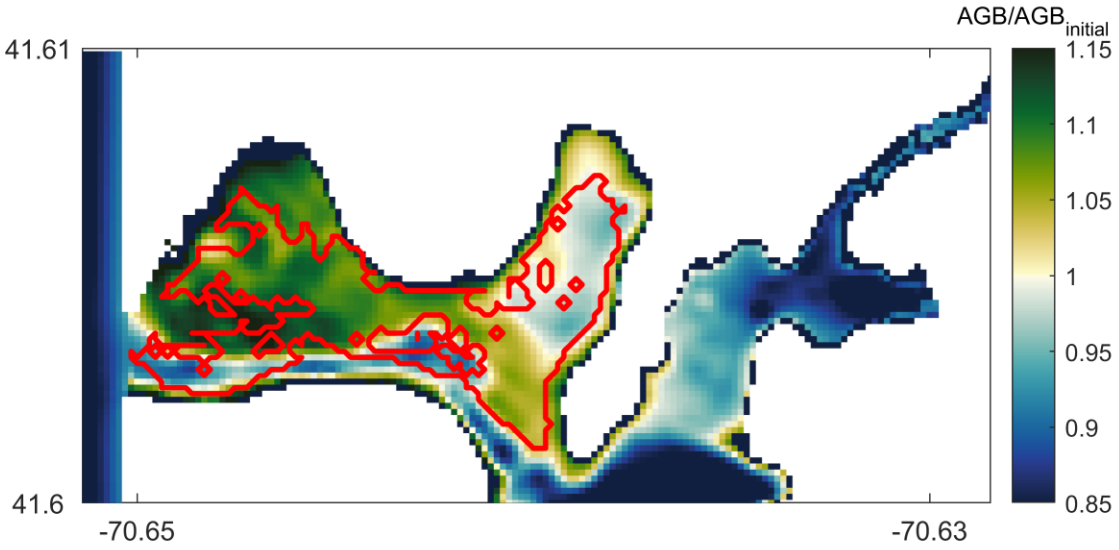

Fig 11: Modeled $AGB/AGB_{initial}$ (above ground biomass) distribution compared with field data showing seagrass coverage extent (red solid line). Values of $AGB/AGB_{initial} > 1$ represent seagrass growth potential and below 1 indicate potential seagrass decline at day 14 of the simulation.

References:

Chassignet, E.P., Arango, H.G., Dietrich, D., Ezer, T., Ghil, M., Haidvogel, D.B., Ma, C.-C., Mehra, A., Paiva, A.M., Sirkes, Z. Dynamics of Atmospheres and Oceans 2000, Vol. 32, pp. 155-183.

Cossarini, G., Querin, S., Solidoro, C., Sannino, G., Lazzari, P., Biagio, V. and Bolzon, G., Development of BFMCOUPLER (v1.0), the coupling scheme that links the MITgcm and BFM models for ocean biogeochemistry simulations, Geosci. Model Dev., 10, 1423–1445, https://doi.org/10.5194/gmd-10-1423-2017, 2017

Costello, C.T. and Kenworthy, W.J., Twelve-Year Mapping and Change Analysis of Eelgrass (Zostera marina) Areal Abundance in Massachusetts (USA) Identifies Statewide Declines, Estuaries and Coasts, Vol, 34:232–242, 2011.

Haidvogel, D.B., Arango, H.G., Hedstrom, K., Beckmann, A., Malanotte-Rizzoli, P., Shchepetkin, A.F. Model evaluation experiments in the North Atlantic Basin: simulations in nonlinear terrain-following coordinates. Dynamics of Atmosphere Oceans 2000, Vol. 32, pp. 239–281.

Haidvogel, D.B., Arango, H.G., Budgell, W.P., Cornuelle, B.D., Churchitser, E., Di Lorenzo, E., Fennel, K., Geyer, W.R., Hermann, A.J., Lanerolle, L., Levin, J., McWilliams, J.C., Miller, A.J., Moore, A.M., Powell, T.M., Shchepetkin, A.F., Sherwood, C.R., Signell, R.P., Warner, J.C., Wilkin, J. Ocean forecasting in terrain following coordinates: Formulation and skill assessment of the Regional Ocean Modeling System. Journal of Computational Physics 2008, Vol. 227, pp. 3595-3624.

Hauxwell, J., Cebrian, J., and Valiela, I., Eelgrass Zostera marina loss in temperate estuaries: relationship to land-derived nitrogen loads and effect of light limitation imposed by algae, Vol.247:59-73, 2003.

Matsumoto, K., Tokos, K., Huston, A., and Joy-Warren, H.: MESMO 2: a mechanistic marine silica cycle and coupling to a simple terrestrial scheme, Geosci. Model Dev., 6, 477–494, https://doi.org/10.5194/gmd-6-477-2013, 2013.

Madden, C.J., Kemp, W.M. Ecosystem model of an estuarine submersed plant community: Calibration and simulation of eutrophication responses. *Estuaries* 19, 457–474 (1996). https://doi.org/10.2307/1352463

Kalra, T.S.; Li, X.; Warner, J.C.; Geyer, W.R.; Wu, H. Comparison of Physical to Numerical Mixing with Different Tracer Advection Schemes in Estuarine Environments. Journal of Marine Science and Engineering 2019, Vol. *7*, 338.

Shchepetkin, A.F., and McWilliams, J.C. The Regional Ocean Modeling System: A split-explicit, free-surface, topography-following coordinates ocean model, Journal of Ocean Modelling 2005, Vol. 9, pp. 347–404.

Shchepetkin, A.F., McWilliams, J.C., Computational Kernel Algorithms for Fine-Scale, Multiprocess, Longtime Oceanic Simulations, Handbook of Numerical Analysis 14, 121-183, 2009.

Sherwood, C.R., Aretxabaleta, A.L., Harris, C.K., Rinehimer, J.P., Verney, R., and Ferré, B., Cohesive and mixed sediment in the Regional Ocean Modeling System (ROMS v3.6) implemented in the Coupled Ocean–Atmosphere–Wave–Sediment Transport Modeling System (COAWST r1234), Geosci. Model Dev., 11, 1849–1871, https://doi.org/10.5194/gmd-11-1849-2018, 2018

Smolarkiewicz, P.K. A fully multidimensional positive definite advection transport algorithm with small implicit diffusion. Journal of Computational Physics 1984, Vol. 54, pp. 325–362.

Woodward, P., and Colella, P., The numerical simulation of two-dimensional fluid flow with strong shocks. Vol.54(1), pp. 115-173, 1984.